Diffraction of interfering waves: two optical beams in the Fresnel region

M.A. Cervantes and E.V. Kurmyshev
Universidad de Sonora, Centro de Investigación en Física
Apartado postal 5-088, 83190 Hermosillo, Sonora, Mexico

Recibido el 3 de diciembre de 1996; aceptado el 8 de septiembre de 1997

In this work we analyze the diffraction of two interfered beams of light by a straight edge opaque screen in the Fresnel approximation. Closed analytical solutions of the considered problem are constructed. A detailed analysis, based on these solutions, has demonstrated interesting and unusual effects that show a considerable interaction between interference and diffraction. The possibility of controlling diffraction by means of interference is explored. The results of diffraction experiments are in a good agreement with those of the theoretical analysis.

Keywords: Difraction, interference, edge and boundary effects

En este tabajo analizamos la difracción de dos haces de luz interferidos producida por una pantalla opaca con un filo recto en la aproximación de Fresnel. Se construyen soluciones analíticas cerradas de este problema. Un análisis detallado basado en estas soluciones revela efectos interesantes y poco usuales que muestran una considerable interacción entre estos dos efectos fundamentales. Se explora la posiblidad de controlar la difracción por medio de interferencia. Los resultados experimentales concuerdan con el análisis teórico en buena medida.

Descriptores: Difracción, interferencia, efectos de borde y de frontera

PACS: 42.25.Fx; 42.25.Hz; 42.25.Gy

1. Introduction

When light propagates through a homogeneous, linear, and isotropic medium, the two effects which influence most the light intensity distribution in a particular region of space are diffraction and interference. [1–4]. The problem of controlling these two effects, and their mutual influence is of considerable theoretical and practical interest for they underlie a lot of technological developments. Well known examples are Fourier optics, holography, holographic interferometry. Diffraction is traditionally considered as an undesired effect for it causes spatial spreading and fringing of the useful radiant energy in optical instrumentation. These two artifacts are known to constrain ultimately the resolving power of optical instruments setting a fundamental limit to their performance.

On the other hand, the study of interference of waves has given rise to the field of interferometry whose importance in modern science is very well established [2].

In this report, we consider the basic experiment and theoretical analysis of diffraction by an opaque screen with a straight edge. Instead of the usual single wave illumination, we assume that the field is in the form of two plane wavefronts mutually coherent. The interfered incident field has cosinusoidal variations of amplitude whose period depends on the angle between the wave vectors of the primary beams, and the wavelength of the light employed. The diffracting screen is so positioned that the edge is parallel to the intersection line between the two plane wavefronts.

Closely related to this problem is the simpler situation posed by the diffraction by a straight edge of a *single* Gaussian or convergent beam which has been treated in the literature [5–10].

Our analysis is based on the theory of Rayleigh and Sommerfeld (see, for example, Refs. 3 and 1). The medium of propagation is considered homogeneous, isotropic and linear. The incident field was assumed to have s-polarized plane infinite wavefronts with unit amplitude in one case and with a Gaussian amplitude profile in the other. The observation screen is located at a distance z from the edge such that the Fresnel approximation is valid. We derive a closed form analytical solution, which allow us to perform a detailed analysis of the considered problem in a wide range of parameters and find out interesting effects produced by mutual influence of diffraction and interference.

The organization of the paper is as follows. In Sect. 2 we pose the problems and solve them in closed analytical forms followed by a graphical analysis of diffraction patterns. We consider the case of plane wavefronts in two cases: In Subsect. 2.2 with uniform amplitude distributions, and in Subsect. 2.3 the case with Gaussian amplitude profiles. In Sect. 3 we present the results of the experiment for the case of Gaussian beams. The main results of the paper are summarized in Sect. 4.

2. Theoretical consideration of diffraction

2.1. Mathematical preliminaries

A Cartesian coordinate system (x_0, y_0, z) is attached to the observation plane with the axes parallel to those of the (x_1, y_1, z) system on the diffracting screen. We use the Rayleigh-Sommerfeld formulation of diffraction by a plane screen (see, for example Refs. 1, 3 and 4). Thus, the observed complex field is given by the well known Fresnel formula

$$\mathbf{E}(x_0, y_0 \mid z) = \frac{\exp(ikz)}{i\lambda z} \iint_{-\infty}^{\infty} \mathbf{E}(x_1, y_1) \exp\left\{ i \frac{k}{2z} \left[(x_0 - x_1)^2 + (y_0 - y_1)^2 \right] \right\} dx_1 dy_1 , \quad (1)$$

where λ is the wavelength of the incident monochromatic field, and $k = 2\pi/\lambda$ is the wave number. The integral in Eq. (1) has been written with infinite limits, taking into account that $\mathbf{E}(x_1, y_1)$ is identically zero outside the aperture in accordance with the Kirchhoff boundary conditions. This integral representation is used here as the basis for our study. Elsewhere in this work we consider the diffracting screen to be posed in the $x_1 y_1$ plane in such a way that the edge coincides with the y_1 axis.

2.2. Fresnel diffraction of interfering uniform waves

2.2.1. *Diffraction of a plane wave at an arbitrary angle of incidence*

If a plane monochromatic wave is incident at an angle θ with respect to the z axis on the screen, its wave vector $\mathbf{k} = (k_x, 0, k_z)$ has only two nonzero components $k_x = k \sin\theta$ and $k_z = k \cos\theta$. The incident field, in the semi-space $z < 0$, is given by

$$\tilde{\mathbf{E}}(\mathbf{r}) \exp(-i\omega t) = \exp(ik_x x_1) \exp(ik_z z) \times \exp(i\alpha) \exp(-i\omega t) , \quad (2)$$

where $\exp(-i\omega t)$ is a time dependent harmonic factor, α is an initial phase and $\mathbf{r} = (x_1, y_1, z)$. In accordance with the Kirchhoff boundary conditions the amplitude distribution of the light field immediately behind the aperture, at $z = +0$, may be written as follows:

$$\tilde{\mathbf{E}}(x_1) = \Theta(x) \exp(ik_x x_1) \exp(i\alpha) , \quad (3)$$

where $\Theta(x)$ is the step function. The amplitude function $\tilde{\mathbf{E}}(x_1)$ being substituted for $\mathbf{E}(x_1, y_1)$ in Eq.(1) leads to the following expression for the Fresnel diffraction pattern:

$$\tilde{\mathbf{E}}(x_0 \mid z, \theta) = \Lambda \frac{1}{2}(1+i) \times \left[\frac{1}{2}(1+i) + C(\xi_1) + iS(\xi_1) \right] , \quad (4)$$

where $C(\xi)$ and $S(\xi)$ are the Fresnel functions, and the phase factor Λ and the variable ξ_1 are given by the following expressions:

$$\Lambda = -i \exp[ik(z + x_0 \sin\theta)] \times \exp\left(\frac{-ikz \sin^2\theta}{2} \right) \exp(i\alpha) , \quad (5)$$

$$\xi_1 = \sqrt{\frac{k}{\pi z}} (x_0 - z \sin\theta) . \quad (6)$$

The intensity distribution of the diffracted field $\tilde{\mathbf{I}}(x_0 \mid z, \theta) = \left| \tilde{\mathbf{E}}(x_0 \mid z, \theta) \right|^2$ is given by

$$\tilde{\mathbf{I}}(x_0 \mid z, \theta) = \frac{1}{2} \left\{ \left[\frac{1}{2} + C(\xi_1) \right]^2 + \left[\frac{1}{2} + S(\xi_1) \right]^2 \right\} . \quad (7)$$

The well known result follows from Eq. (7), that is, in the case of θ-incident wave the fringe pattern at a distance z is equal to the pattern of normally incident wave, but displaced at the distance $z \sin\theta$ along the x_0 axis.

2.2.2. *Solution of the diffraction problem for two interfered plane waves*

We consider the diffraction of two interfering plane waves, one of which is normally incident and the other is incident at an angle θ. The amplitude distribution of the two interfered waves is the following one:

$$\mathbf{E}(\mathbf{r}) = 2 \cos\left[\frac{(k_z - k) z + k x_1 \sin\theta + \alpha}{2} \right] \times \exp\left[i \frac{(k_z + k) z + k x_1 \sin\theta + \alpha}{2} \right] . \quad (8)$$

The amplitude and intensity distributions of the interfered field in the plane of the screen are as follows:

$$\mathbf{E}(\mathbf{r}) \mid_{z=0} = 2 \cos\left(\frac{k x_1 \sin\theta + \alpha}{2} \right) \times \exp\left(i \frac{k x_1 \sin\theta + \alpha}{2} \right) , \quad (9)$$

$$\mathbf{I}(x_1, y_1) = |\mathbf{E}(\mathbf{r})|^2_{z=0} = 4 \cos^2\left(\frac{k x_1 \sin\theta + \alpha}{2} \right) . \quad (10)$$

The intensity distribution Eq. (10) has the well known $\cos^2$-modulation. Varying the initial phase α allows us to position any region of the $\cos^2$-wave at the edge of the screen. The fringes are separated by the distance $\delta_x = \lambda / \sin\theta \simeq \lambda/\theta$. We used the condition $\theta \ll 1$. This is because as θ increases, the fringe spacing decreases making the positioning of the edge with respect to the fringe position more critical and making the experiment more vulnerable to equipment imperfections. Thus, the fringe density was kept comfortably low so that the available positioning equipment permitted us to place the elements with reliable reproducibility both linearly or angularly. This necessarily means that we have to work with small angles of interference θ.

In principle, the solution of the considered diffraction problem is formally obtained by integrating Eq. (1) with the Kirchhoff boundary condition for the incident field, [Eq. (9)], but we can invoke the principle of linear superposition for diffracted fields and use Eqs. (4), (5), and (6). Thus, the amplitude diffraction pattern of the two interfering plane waves is as follows:

$$\mathbf{E}(x_0, y_0 \mid z) = \frac{\exp(ikz)}{i\lambda z}\int_{-\infty}^{\infty}\exp\left(i\frac{k}{2z}(y_0-y_1)^2\right)dy_1\exp\left(i\frac{kx_1\sin\theta+\alpha}{2}\right)\exp\left[i\frac{k}{2z}(x_0-x_1)^2\right]dx_1$$

$$= \frac{1}{2}(1-i)\exp(ikz)\left[\frac{1}{2}(1+i)+C\left(\tilde{\xi}_1\right)+iS\left(\tilde{\xi}_1\right)\right]+\Lambda\frac{1}{2}(1+i)\left[\frac{1}{2}(1+i)+C(\xi_1)+iS(\xi_1)\right], \quad (11)$$

where the factor Λ is given by Eq. (5), the variable $\tilde{\xi}_1 = \xi_1 \mid_{\theta=0} = \sqrt{k/(\pi z)}x_0$ and the variable ξ_1 is given by Eq. (6). The intensity field follows from Eq. (11):

$$\mathbf{I}(x_0, y_0 \mid z) = |\mathbf{E}(x_0, y_0 \mid z)|^2 = \tilde{\mathbf{I}}(x_0 \mid z, 0) + \tilde{\mathbf{I}}(x_0 \mid z, \theta) + \mathbf{CT}, \quad (12)$$

where intensities of interfering plane waves are correspondingly given by the following expressions

$$\tilde{\mathbf{I}}(x_0 \mid z, \theta) = \frac{1}{2}\left\{\left[\frac{1}{2}+C(\xi_1)\right]^2+\left[\frac{1}{2}+S(\xi_1)\right]^2\right\}, \quad (13)$$

$$\tilde{\mathbf{I}}(x_0 \mid z, 0) = \frac{1}{2}\left\{\left[\frac{1}{2}+C\left(\tilde{\xi}_1\right)\right]^2+\left[\frac{1}{2}+S\left(\tilde{\xi}_1\right)\right]^2\right\}, \quad (14)$$

and the cross term $\mathbf{CT}$ is:

$$\mathbf{CT} = \cos\left[k\left(x_0-\frac{z\sin\theta}{2}\right)\sin\theta+\alpha\right]\left\{\left[\frac{1}{2}+C\left(\tilde{\xi}_1\right)\right]\left[\frac{1}{2}+C(\xi_1)\right]+\left[\frac{1}{2}+S\left(\tilde{\xi}_1\right)\right]\left[\frac{1}{2}+S(\xi_1)\right]\right\}$$

$$-\sin\left[k\left(x_0-\frac{z\sin\theta}{2}\right)\sin\theta+\alpha\right]\left\{\left[\frac{1}{2}+C\left(\tilde{\xi}_1\right)\right]\left[\frac{1}{2}+S(\xi_1)\right]-\left[\frac{1}{2}+S\left(\tilde{\xi}_1\right)\right]\left[\frac{1}{2}+C(\xi_1)\right]\right\}. \quad (15)$$

The structural representation of the diffracted field, [Eqs. (12)–(15)], provides an insight of the mutual interaction between diffraction and interference. To see it in more details we made graphical simulation of these formulas.

2.2.3. *Diffraction pattern as a function of interference angle at different positions of the diffracting edge*

Two important parameters in the considered problem are the fringe separation $\delta_x = \lambda/\sin\theta \simeq \lambda/\theta$, before diffraction takes place, and the position of the geometrical shadow in the observation plane for the θ-incident wave, $d_x = z\sin\theta \simeq z\theta$. We expect, with regard to angle θ, that the diffraction pattern will behave in a different manner for θ such that the pure interference fringe separation, δ_x, be greater, comparable or smaller than the first diffraction peak of a normally incident single plane wave. Accordingly, the following values $\theta = 10^{-5}, 10^{-4}, 2\times10^{-4}, 10^{-3}$ rad were considered to be representative. Nevertheless, a large number of curves were drawn to verify the selection of the above angle values.

The two sets of intensity distribution of diffracted fields along the x_0-axis, [Eqs. (12)–(15)], which correspond to two different positions of the diffracting edge with respect to the fringe pattern, are graphically analyzed.

The diffraction patterns, [Eqs. (12)–(15)], are shown in Fig. 1 with the thick solid line for the case $\alpha = 0$ (*i.e.*, the center of a bright fringe coincides with the edge), and $z = 4$ m. The sequence of four thick solid line plots (see Figs. 1a–1d) for $\theta = 10^{-5}, 10^{-4}, 2\times10^{-4}, 10^{-3}$ rad contain diffraction effects, whereas the corresponding pure interference patterns, obtained in the absence of the screen, are given in the thin solid line. The undiffracted interference patterns in the observation plane are used as reference of changes caused by diffraction. They are shifted along the x_0- axis by the distance $x_0 = z(1-\cos\theta)/\sin\theta \simeq z\theta/2$ with respect to that in the plane of the screen in accordance with Eq. (8). The wavelength used for the calculations and the one used in our experiments is $\lambda = 594$ nm, which corresponds to a yellow line of a He Ne laser.

Two principal observations can be made on the basis of graphical analysis.

1. If angle θ is large enough, such that the relation $d_x/\delta_x = z\theta^2/\lambda \gg 1$ is valid, then three qualitatively different zones can be distinguished in the patterns given by Eq. (12) (see, for example, Fig. 1d). In the first zone from -1 to 2.5 mm we observe a diffraction pattern of a single normally incident wave slightly

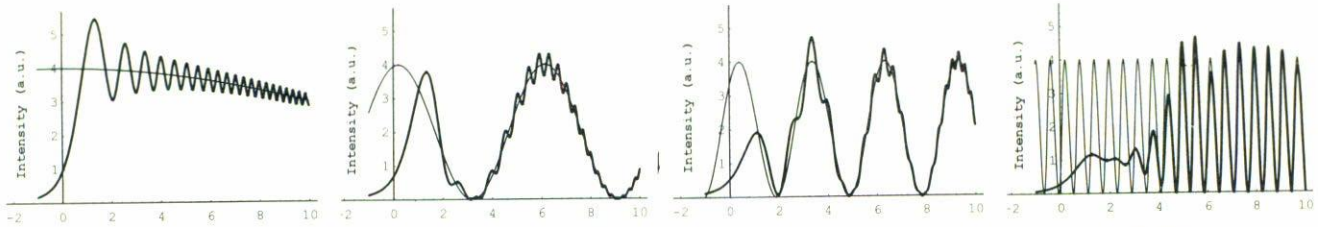

FIGURE 1. Diffraction pattern of two uniform interfered plane waves I. The thick curve is the diffracted field intensity and the thin one is the field intensity in the absence of the diffracting screen. The initial phase is $\alpha = 0$, meaning a peak of intensity is made to coincide with the edge at $z = 0$, *i.e.* on the (x_1, y_1) plane. The plots (a) through (d) in this figure (and in Figs. 2 to 4), correspond to the values of the interference angle (a): $\theta = 10^{-5}$, (b): $\theta = 10^{-4}$, (c): $\theta = 2 \times 10^{-4}$, (d): $\theta = 10^{-3}$ rad, respectively. The parameters $\delta_x = \lambda/\theta$ and $d_x = z\theta$ take on correspondingly the values $\delta_x = 5.94 \times (10^{-2}, 10^{-3}, 0.5 \times 10^{-3}, 10^{-4})$ m and $d_x = 4 \times (10^{-5}, 10^{-4}, 2 \times 10^{-4}, 10^{-3})$ m.

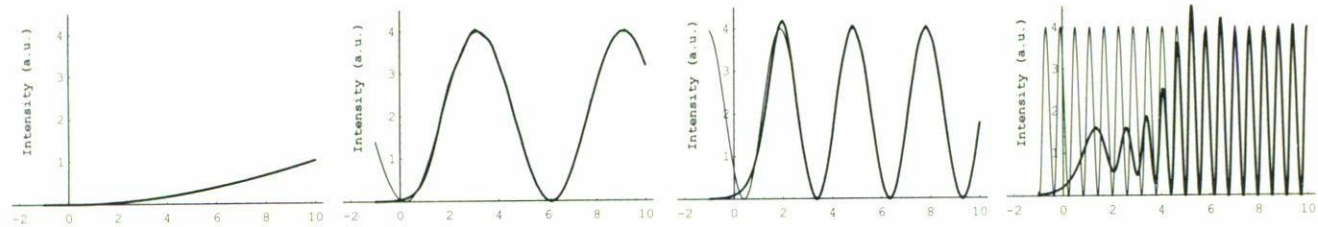

FIGURE 2. Diffraction pattern of two uniform interfered plane waves II. The same conditions as I, except for the initial phase is $\alpha = \pi$, meaning a zero intensity fringe is located at the edge.

deformed by the presence of the wing of the θ-incident wave. This zone is followed by a region (from 2.5 to 6 mm in the x_0 axis) of a strong interaction between diffraction and interference. Finally, there is a region where interference dominates diffraction (for $x_0 \geq 6$ mm), where the fringe intensity is near to that obtained if only interference were considered.

2. For angles near $\theta = 10^{-4}$ rad the diffraction pattern exhibits a unique smooth peak from -1 to 2 mm (see the first peak in Figs. 1b and 1c). An interesting feature is that the fringe does not exhibits the ripple of diffraction-like fringes shown in the next interval from 2 to 10 mm. We think that the latter is a consequence of a comparable mutual influence of the two phenomena. Figures 1b and 1c show how diffraction-like fringes modulate the peaks of the interference-like fringes.

Figure 1a, shows that at small values of the interference angle θ, when the width of an interference fringe is large enough, the diffraction pattern of interfered waves almost coincides with that of a single plane wave of double amplitude. An increase of θ causes, at the beginning, small deformation of the diffraction pattern and then the evolution of the diffraction pattern becomes more complicated, leading to the effects described above.

Figure 2 presents the calculated fields for the case $\alpha = \pi$ (*i.e.*, the center of a zero intensity fringe coincides with the edge of the screen). The rest of the parameters and the distribution of plots are kept equal to those of Fig. 1.

Analyzing the diffraction of interfered waves with a phase difference $\alpha = \pi$, we find it to be similar to that for the case $\alpha = 0$. For the angle $\theta = 10^{-3}$ rad, the diffraction pattern, presented by the thick solid line Fig. 2d, is not identical to that of Fig. 1d, but has the same general structure. In both situations we can distinguish three regions: in the region of geometrical shadow of the θ-incident wave there is a predominant diffraction of single plane wave, then follows a transition zone followed by the region, where the interference pattern is subject to a marginal diffraction effect.

The differences between the two cases ($\alpha = 0$ and $\alpha = \pi$) become apparent for small values of θ. In the case $\alpha = \pi$ and the rather small $\theta \leq 2 \times 10^{-4}$ rad (see thick solid line in Figs. 2a–2c), a diffraction pattern closely follows the corresponding interference pattern, thin solid line in Figs. 2a–2c. As a matter of fact, Fig. 2a includes both curves superimposed, appearing as a single plot. This does not take place when $\alpha = 0$. A further increment of θ reduces the fringe spacing, and in turn causes considerable penetration

of the diffracted field in the region of geometrical shadow, Figs. 2b–2d. If $\theta \gg 10^{-4}$ rad, then the diffraction patterns for $\alpha = 0$ and $\alpha = \pi$ have similar structures, as it was described above. Thus, we can conclude that there always exists a critical interference angle θ (in our case $\theta_c \sim 10^{-4}$ rad) such that, in the vicinity of this value, a diffraction pattern of interfered waves is subject to qualitative changes when θ varies.

2.3. Diffraction of interfering Gaussian beams

A more realistic illumination than that represented by ideal infinite plane wavefronts is that provided by beams of light produced by lasers. Particularly convenient are those which are characterized by a field with an intensity profile of Gaussian type. This can be better described as the TEM_{00} laser mode. Following the accepted theory of optical resonators, [12, 13, 15–17], we presume that the normally incident beam possess a field amplitude distribution of Gaussian type.

$$\tilde{\mathbf{E}}_1(\mathbf{r}) \exp(-i\omega t) = A \frac{w_0}{w(z')} \exp\left\{-\left[(x-x_1)^2 + (y-y_1)^2\right]\left[\frac{1}{w^2(z')} + \frac{ik}{2R(z')}\right]\right\} \exp\{i[kz' + \eta(z')]\} \exp(-i\omega t). \quad (16)$$

Here A is the amplitude considered constant, and $w(z')$ is the z'-dependent semi-width of the beam defined as

$$w^2(z') = w_0^2\left[1 + \left(\frac{\lambda z'}{\pi w_0^2 n}\right)^2\right] = w_0^2\left[1 + \left(\frac{z'}{z_0}\right)^2\right], \quad (17)$$

where w_0 is the minimum spot size, which is the beam spot size at the plane $z' = 0$. The phase $\eta(z') = \arctan(z'/z_0)$. The center of the beam is located at the point (x_1, y_1) in the (x, y) plane. We take here the semi-width of the beam to be the same in the x and y direction.

Besides the Gaussian amplitude profile such beams of light are characterized by wavefronts with finite radius of curvature, except at the waist where it becomes infinite. The radius of curvature $R(z')$ of the very nearly spherical wavefront at z' is

$$R(z') = z'\left[1 + \left(\frac{z_0}{z'}\right)^2\right], \quad z_0 \equiv \frac{\pi w_0^2 n}{\lambda}, \quad k = \frac{2\pi}{\lambda} n. \quad (18)$$

We estimate here the radius of curvature $R(z')$ for a quite typical laboratory situation when the parameters are supposed to have the following values: $\lambda = 594$ nm, $w_0 = 10^{-2}$ m, and the diffracting screen is distant from the waist plane by $z' = 1$ m. Then we readily find that $k = 2\pi/\lambda \simeq 1.057 \times 10^7 \mathrm{m}^{-1}$, $z_0 = 528.6$ m. Accordingly, $w^2(1) = w_0^2[1 + (1/z_0)^2] = w_0^2(1 + 3.5 \times 10^{-6}) \simeq w_0^2$ and $R(1) = [1 + (z_0)^2] \simeq 2.79 \times 10^5$ m. Moreover, the phase $\eta(1) = \arctan(1/z_0) \simeq 1.89 \times 10^{-3}$ rad.

Keeping in mind that we are going to use the above expression of the laser beam in the diffraction Rayleigh-Sommerfeld integral we also find the value of the term $ikr^2/2R(1) \simeq i18.9\, r^2 < i10^{-2}$. Here we took the radius of the area of a beam spot to be of the order $r \leq 2w_0 = 2 \times 10^{-2}$ m.

In addition, we note that the minimum of the radius of curvature of the fundamental Gaussian beam is equal to $R_{\min} = R(z_0) = 2z_0$ and is located at the distance z_0 from the beam waist. This distance is very large for typical laboratory experiment. Thus, the estimates show that for the diffraction interference experiments under a typical laboratory situation we can safely neglect both the term which contains the radius of curvature and the phase $\eta(z')$. Thus, for the sake of simplicity, we will consider that the beams possess negligible curvature and the phase-fronts are treated as planar [18, 17].

This conditions meet the experiment in the case in which the waists of the incident beams are made to coincide with the plane of the diffracting screen or are subject to collimation, as was the case in our experiments. Under these conditions, the interference pattern of the incident fields is largely determined by the tilt angle of the phase-fronts and not to their curvature, as is the case of interferometers that rely on wavefront shearing to produce a fringe pattern.

Under the conditions described above, the θ-incident Gaussian beam, [Eq. (16)], is reduced to the Gaussian beam with the plane wavefront and, in the plane of the diffracting screen, is given by the following formula:

$$\tilde{\mathbf{E}}(\mathbf{r})\,|_{z=0} = \exp\left[-\frac{(x\cos\theta - x_1\cos\theta)^2 + y^2}{2w^2}\right] \times \exp(ikx\sin\theta + i\alpha), \quad (19)$$

where we omitted the time dependent term $\exp(-i\omega t)$, added an initial phase α term and used the new notation $2w^2 \equiv w_0^2$ =const. The beam has the amplitude $A = 1$, and is centered at $y_1 = 0$.

2.3.1. *Diffraction of a single Gaussian beam*

The diffraction by a semi-infinite plane with a straight edge of a single normally incident Gaussian beam, described by Eq. (16), was reported in Refs. 5 and 10. If the beam, [Eq. (19)], is incident at a small angle θ on a semi-infinite screen, the diffracted beam at the point (x_0, y_0, z) is accordingly given by the closed form analytical solution

$$\tilde{\mathbf{E}}(x_0,y_0 \mid z,x_1,w,\theta) = \frac{\exp(ikz)\exp(i\alpha)}{i\lambda z}\int_{-\infty}^{\infty}\exp\left(-\frac{y^2}{2w^2}\right)\exp\left[i\frac{k}{2z}(y_0-y)^2\right]dy$$
$$\times\int_0^{\infty}\exp\left[-\frac{(x\cos\theta-x_1\cos\theta)^2}{2w^2}\right]\exp(ikx\sin\theta)\exp\left[i\frac{k}{2z}(x_0-x)^2\right]dx$$
$$= \frac{\exp(ikz)\exp(i\alpha)}{i\lambda z} I(y_0 \mid z,w)\, I(x_0 \mid z,x_1,w,\theta), \tag{20}$$

where the integrals I_{y_0} and I_{x_0} are given by (see Ref. 11)

$$I(y_0 \mid z,w) = \frac{\sqrt{\lambda z}}{\left[1+z^2/(k^2w^4)\right]^{1/4}}\exp\left\{-\frac{y_0^2}{2w^2\left[1+z^2/(k^2w^4)\right]}\right\}$$
$$\times\exp\left\{i\left[\frac{1}{2}\arctan\left(\frac{kw}{z}\right)+\frac{y_0^2}{2w^2\left[(kw^2)/z+z/(kw^2)\right]}\right]\right\}, \tag{21}$$

$$I(x_0 \mid z,x_1,w,\theta) = \sqrt{\pi\beta}\left[1-\Phi\left(\gamma\sqrt{\beta}\right)\right]\exp\left[-\frac{\cos^2\theta}{2w^2}\left(1+\frac{z^2\cos^4\theta}{k^2w^4}\right)^{-1}(x_0-x_1-z\sin\theta)^2\right]$$
$$\times\exp\left\{i\left[kx_0\sin\theta-\frac{1}{2}kz\sin^2\theta+\frac{k}{2z}\left(1+\frac{k^2w^4}{z^2\cos^4\theta}\right)^{-1}(x_0-x_1-z\sin\theta)^2\right]\right\}. \tag{22}$$

The parameter β and the variable γ are defined by the following expressions

$$\beta = \frac{z}{2k}\left(\frac{z\cos^2\theta}{kw^2}-i\right)^{-1}, \qquad \gamma = \frac{ikx_0}{z}-ik\sin\theta-\frac{x_1\cos^2\theta}{w^2}. \tag{23}$$

Using Eqs. (20)–(23), the intensity distribution of the diffracted Gaussian beam is readily obtained:

$$\tilde{\mathbf{I}}(x_0,y_0 \mid z,x_1,w,\theta) = \left|\tilde{\mathbf{E}}(x_0,y_0 \mid z,x_1,w,\theta)\right|^2$$
$$= \frac{1}{4}\left(1+\frac{z^2}{k^2w^4}\right)^{-1/2}\left(1+\frac{z^2\cos^4\theta}{k^2w^4}\right)^{-1/2}$$
$$\times\exp\left\{-\frac{y_0^2}{w^2\left[1+z^2/(k^2w^4)\right]}\right\}\left[1-\Phi\left(\gamma\sqrt{\beta}\right)\right]\left[1-\Phi^*\left(\gamma\sqrt{\beta}\right)\right]$$
$$\times\exp\left[-\frac{\cos^2\theta}{w^2}\left(1+\frac{z^2\cos^4\theta}{k^2w^4}\right)^{-1}(x_0-x_1-z\sin\theta)^2\right], \tag{24}$$

where $\Phi^*\left(\gamma\sqrt{\beta}\right)$ is the complex conjugate of the error function $\Phi\left(\gamma\sqrt{\beta}\right)$. This distribution is separable in variables x_0 and y_0. The particular case of a normally incident Gaussian beam is obtained from Eqs. (23)–(24) for $\theta = 0$:

$$\tilde{\mathbf{I}}(x_0,y_0 \mid z,x_1,w,0) = \frac{1}{4}\left(1+\frac{z^2}{k^2w^4}\right)^{-1}\exp\left[-\frac{y_0^2}{w^2\left(1+z^2/k^2w^4\right)}\right]$$
$$\times\left[1-\Phi\left(\gamma\sqrt{\beta}\right)\right]\left[1-\Phi^*\left(\gamma\sqrt{\beta}\right)\right]\exp\left[-\frac{1}{w^2}\left(1+\frac{z^2}{k^2w^4}\right)^{-1}(x_0-x_1)^2\right]. \tag{25}$$

From Eqs. (24) and (25) it can be seen that, in addition to the well known spreading of a Gaussian beam with the distance z, the center of the Gaussian envelope (crossing the plane of diffracting screen at the point $x = x_1$) will propagate along the geometrical ray $x = x_1 + z\sin\theta$. This ray crosses the observation plane x_0y_0, which is located at a distance z from the diffraction screen, at the point $x_0 = x_1 + z\sin\theta$ but not at the point $x_0' = x_1 + z\tan\theta$ as it were in the case if the beam was freely propagating without diffraction. Since $|\sin\theta| < |\tan\theta|$, the value $x_0 < x_0'$ for positive angles θ, and $x_0 > x_0'$ for negative angles. Thus, the diffracting screen deviates the Gaussian beam in such a way that the Gaussian

envelope moves along a geometrical ray which is closer to the z axis than that of the free beam propagation.

The shape and position of the diffraction fringes are also influenced by the parameter x_1 in combination with the width w through the variable γ. When w tends to ∞ the combination x_1/w tends to 0, that is, the influence of the parameter x_1 is diminished. To be more precise, let us give an estimate of the parameters for the experiment which we describe below when one has $\lambda = 594$ nm, the distance from the diffracting screen to the observation plane is $z = 4$ m, $w = 0.5 \times 10^{-2}$ m, $x_1 \leq 0.5 \times 10^{-2}$ m, $\theta \leq 10^{-3}$ rad. The wave number is $k \simeq 1.057 \cdot 10^7$ m^{-1}. Then, the combination $z^2/\left(kw^2\right)^2 \sim 2 \times 10^{-4}$, which defines the spreading of a Gaussian beam, is very small. The ratio $k/z \approx 0.266 \times 10^7$ m^{-2}, in the variable γ, [Eq. (23)], is very large. This makes the influence of the combination x_1/w^2 relatively small in the variable γ. Thus, the parameters x_1 and w manifest themselves in a diffraction pattern of a single Gaussian beam mainly through the Gaussian envelope.

2.3.2. Diffraction pattern of two interfering Gaussian beams: explicit analytical solution and graphical analysis

With the above given results we can study the diffraction pattern of a light field produced by the interference of two Gaussian beams. We take one beam to be θ-incident, [Eq. (19)], and the other to be normally incident beam, Eq. (19) at $\theta = 0$ and $\alpha = 0$. The beams have equal semi-width w, the amplitudes equal to $A = 1$. The centers of beams are considered to coincide with each other in the plane of the diffracting screen. The interference pattern produced by the beams in the plane of the diffraction screen is as follows:

$$\mathbf{E}\left(\mathbf{r}\right)|_{z=0} = 2\exp\left(-\frac{y^2}{2w^2}\right)\exp\left[-\frac{\left(x-x_1\right)^2}{2w^2}\right] \times \exp\left[\frac{i\left(kx\sin\theta+\alpha\right)}{2}\right]\cos\left[\frac{\left(kx\sin\theta+\alpha\right)}{2}\right]. \tag{26}$$

In Eq. (26) we took into account a small value of the interference angle θ, the last expression is valid within $\mathcal{O}(\theta^2)$. The intensity distribution of interfering Gaussian beams exhibits commonly known $\cos^2$-fringes modified by the Gaussian envelope as follows:

$$\mathbf{I}\left(x,y\right) = \left|\mathbf{E}\left(\mathbf{r}\right)\right|^2_{z=0} = 4\exp\left(-\frac{y^2}{w^2}\right)\exp\left[-\frac{\left(x-x_1\right)^2}{w^2}\right] \times \cos^2\left[\left(kx\sin\theta+\alpha\right)/2\right]. \tag{27}$$

In the Fresnel approximation the amplitude diffraction pattern of the two interfered Gaussian beams by a semi-infinite screen positioned in the xy-plane with the straight edge along the y-axis is as follows:

$$\begin{aligned}\mathbf{E}(x_0,y_0 \mid z,x_1,w,\theta,\alpha) &= 2\frac{\exp(ikz)}{i\lambda z}\int_{-\infty}^{\infty}\exp\left(-\frac{y^2}{2w}\right)\exp\left[i\frac{k}{2z}(y_0-y)^2\right]dy \\ &\times\int_0^{\infty}\exp\left[-\frac{\left(x-x_1\right)^2}{2w^2}\right]\exp\left[\frac{i\left(kx\sin\theta+\alpha\right)}{2}\right]\cos\left[\frac{\left(kx\sin\theta+\alpha\right)}{2}\right]\exp\left[i\frac{k}{2z}\left(x_0-x\right)^2\right]dx \\ &\simeq \frac{\exp(ikz)}{i\lambda z}I\left(y_0 \mid z,w\right)\left[\exp\left(i\alpha\right)I\left(x_0 \mid z,x_1,w,\theta\right)+I\left(x_0 \mid z,x_1,w,0\right)\right], \end{aligned} \tag{28}$$

where the integral $I\left(y_0 \mid z,w\right)$ is given by Eq. (21), and the integral $I\left(x_0 \mid z,x_1,w,\theta\right)$is given by Eqs. (22)–(23). Then, the intensity distribution of the diffraction pattern is calculated as follows:

$$\begin{aligned}\mathbf{I}(x_0,y_0 \mid z,x_1,w,\theta,\alpha) &= \left|\mathbf{E}(x_0,y_0 \mid z,x_1,w,\theta,\alpha)\right|^2 \\ &= \tilde{\mathbf{I}}\left(x_0,y_0 \mid z,x_1,w,\theta\right)+\tilde{\mathbf{I}}\left(x_0,y_0 \mid z,x_1,w,0\right)+\mathbf{CT}\left(x_0,y_0 \mid z,x_1,w,\theta,\alpha\right). \end{aligned} \tag{29}$$

The intensity distribution of the diffraction pattern of a single Gaussian beam $\tilde{\mathbf{I}}\left(x_0,y_0 \mid z,x_1,w,\theta\right)$ is given by Eq. (24), and the cross term $\mathbf{CT}\left(x_0,y_0 \mid z,x_1,w,\theta,\alpha\right)$ is given by the following expression:

$$\begin{aligned}\mathbf{CT}\left(x_0,y_0 \mid z,x_1,w,\theta,\alpha\right) =& \frac{1}{2}\left(1+\frac{z^2}{k^2w^4}\right)^{-1/2}\exp\left\{-\frac{y_0^2}{w^2\left[1+z^2/\left(k^2w^4\right)\right]}\right\} \\ &\times\exp\left[-\frac{\cos^2\theta}{2w^2}\left(1+\frac{z^2\cos^4\theta}{k^2w^4}\right)^{-1}\left(x_0-x_1-z\sin\theta\right)^2\right. \\ &\left.-\frac{1}{2w^2}\left(1+\frac{z^2}{k^2w^4}\right)^{-1}\left(x_0-x_1\right)^2\right]\left(\mathrm{Re}\left[\Psi\right]\cos\phi-\mathrm{Im}\left[\Psi\right]\sin\phi\right). \end{aligned} \tag{30}$$

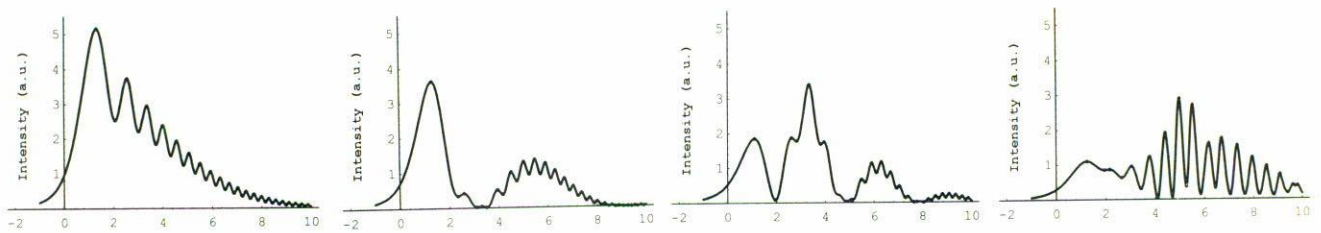

FIGURE 3. Diffraction pattern of two interfered Gaussian beams I. The initial phase $\alpha = 0$. The center of the Gaussian envelope at $x_1 = 0$.

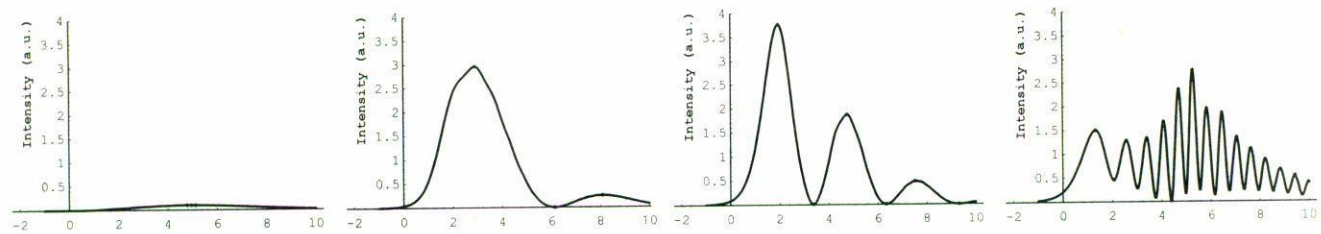

FIGURE 4. Diffraction pattern of two interfered Gaussian beams II. Same conditions as Fig. 3, except the initial phase $\alpha = \pi$.

The function Ψ is given by the expression

$$\Psi\left(x_0, y_0 \mid z, x_1, w, \theta\right) = \left(\frac{z\cos^2\theta}{kw^2} - i\right)^{-1/2} \left(\frac{z}{kw^2} + i\right)^{-1/2} \left[1 - \Phi\left(\gamma_\theta\sqrt{\beta_\theta}\right)\right]\left[1 - \Phi^*\left(\gamma_0\sqrt{\beta_0}\right)\right], \tag{31}$$

and the angle ϕ is defined by the following expression:

$$\phi = \alpha + kx_0\sin\theta - \frac{1}{2}kz\sin^2\theta + \frac{k}{2z}\left(1 + \frac{k^2w^4}{z^2\cos^4\theta}\right)^{-1}\left(x_0 - x_1 - z\sin\theta\right)^2 - \frac{k}{2z}\left(1 + \frac{k^2w^4}{z^2}\right)^{-1}\left(x_0 - x_1\right)^2. \tag{32}$$

The variables γ_θ, β_θ are defined by Eqs. (23) respectively, and notations γ_0, β_0 correspond to the angle $\theta = 0$.

In order to see the variation of the diffraction pattern of two interfered Gaussian beams we have made a computer simulation of the solution presented by Eq. (29) for the cross-section $y_0 = y_1 = 0$. We kept constant the following parameters: the semi-width of the beams $w = 0.5 \times 10^{-2}$ m, the distance from the diffracting screen to the observation plane $z = 4$ m, the wavelength of light $\lambda = 594$ nm. The center of the interfered Gaussian beam is located at the point $x_1 = 0$ (for Figs. 3 and 4). Note that the initial phase value $\alpha = 0$ corresponds to the case when the center of a bright fringe coincides with the straight edge of the diffracting screen, and the value $\alpha = \pi$ corresponds to the case when the center of a dark fringe (zero intensity) of interfered wave coincides with the edge.

Curves were obtained for a variety of values of θ. However, the same set of values of previous Section are used ($\theta = 10^{-5}, 10^{-4}, 2 \times 10^{-4}, 10^{-3}$ rad) for the sake of comparison, and the curves are shown in Fig. 3 for $\alpha = 0$.

The four plots for $\alpha = \pi$ are presented in Fig. 4.

Examination of the diffraction patterns of two interfered Gaussian beams (Figs. 3–4) and that of the constant amplitude plane waves leads to the conclusion that diffraction patterns of two interfered Gaussian beams vary similarly to that for the constant amplitude plane waves. They differ solely by the Gaussian envelope modulation. This conclusion, although expected, [5] is not obvious, because the corresponding analytical solutions have quite different form and, in addition, in the Gaussian case we have two more parameters to consider, which are the center of the Gaussian envelope x_1 and its semi-width w.

In order to see the dependence of the diffraction pattern on these parameters, we obtained the intensity distribution of the diffracted light as a function of the position of the screen edge with respect to a stationary interference pattern for the given semi-width $w = 0.5 \times 10^{-2}$ m. For this purpose the pair of parameters (x_1, α) were changed simultaneously, and the following values were given for $x_1 = 0, 6 \times 10^{-4}, 10^{-3}, 1.4 \times 10^{-3}, 1.8 \times 10^{-3}, 2 \times 10^{-3}, 2.4 \times 10^{-3}, 3 \times 10^{-3},$

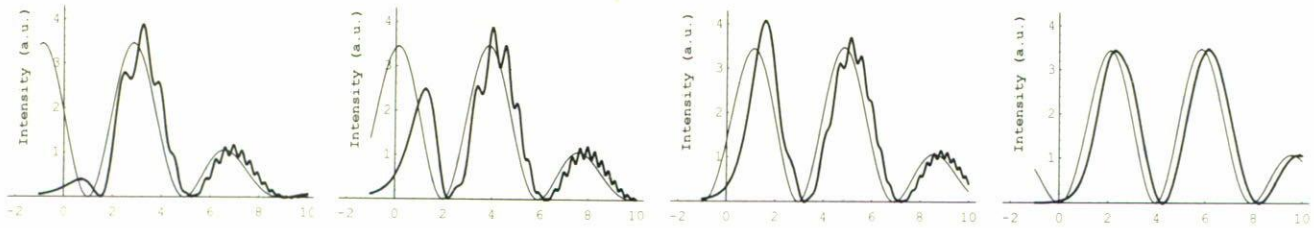

FIGURE 5. Diffraction pattern as a function of the edge position with respect to the interfered Gaussian beam. The pairs of varied parameters are $(x_1, \alpha) = (10^{-3}, \pi/2), (2 \times 10^{-3}, 0), (3 \times 10^{-3}, -\pi/2), (4 \times 10^{-3}, -\pi)$. The interference angle $\theta = 1.5 \times 10^{-4}$ rad.

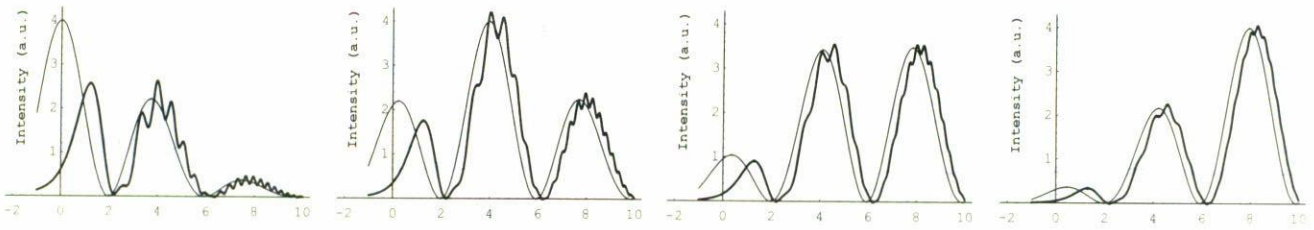

FIGURE 6. Diffraction pattern as a function of the envelope position. The values of the varied parameter are $x_1 = 0, 4 \times 10^{-3}, 6 \times 10^{-3}, 8 \times 10^{-3}$ m. The interference angle $\theta = 1.5 \times 10^{-4}$ rad.

$3.6 \times 10^{-3}, 4 \times 10^{-3}$ m and correspondingly for $\alpha = \pi, 0.7\pi, 0.5\pi, 0.3\pi, 0.1\pi, 0, -0.2\pi, -0.5\pi, -0.8\pi, -\pi$ rad. Four typical diffraction patterns are presented in thick curves in Figs. 5a–5d. The thin curves shown in Figs. 5a–5d represent the corresponding cross-sections, defined by $y = y_1 = 0$, of the incident interfered wave as it is just before the diffraction screen at $z = -0$. An analysis of the curves (see, also Fig. 4) leads to the conclusion that the changes of the diffraction pattern are mainly determined by a position of the interference pattern with respect to the diffraction edge. But, we note that for the pair of parameters $x_1 = 3 \times 10^{-3}$ m and $\alpha = -\pi/2$, an appreciable increase of the intensity of the first bright fringe (nearest to the region of geometrical shadow) occurs (thick curve in Fig. 5c).

In the previous analysis the response of the diffraction pattern for the position of the screen edge with respect to a stationary interference pattern was obtained. We also analyzed the diffracted field when only the envelope of the incident beam was shifted, while the fringe spacing remained unchanged for the particular case in which a maximum of the bright fringe was positioned at the edge of the diffraction screen. This means that we maintained constant $w = 0.5 \times 10^{-2}$ m, $\theta = 1.5 \times 10^{-4}$, $\alpha = 0$ and varied only $x_1 = 0, 2 \times 10^{-3}, 4 \times 10^{-3}, 6 \times 10^{-3}, 8 \times 10^{-3}$ m.

The results are presented in thick curves in Figs. 6a–6d. The thin curves in Figs. 6a–6d give the undiffracted incident interfered beam for $y = y_1 = 0$.

Analyzing of these results we can conclude that the shape of the envelope influences the light pattern mainly as a scaling factor.

3. Experimental

To confirm these results, we set up a two beam interferometer based on the principle of division of amplitude, like a Michelson type, which produces two plane wavefronts that, after interference, are diffracted by a knife edge (see Fig.7). The mirrors are so adjusted that few fringes are displayed across the transverse size of the beam. If the interferometer

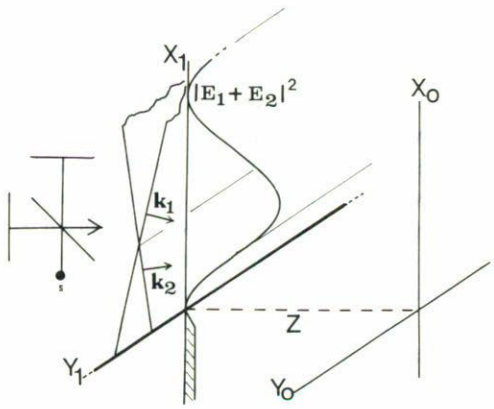

FIGURE 7. Schematic of two interfering plane waves diffracted by a straight edge screen.

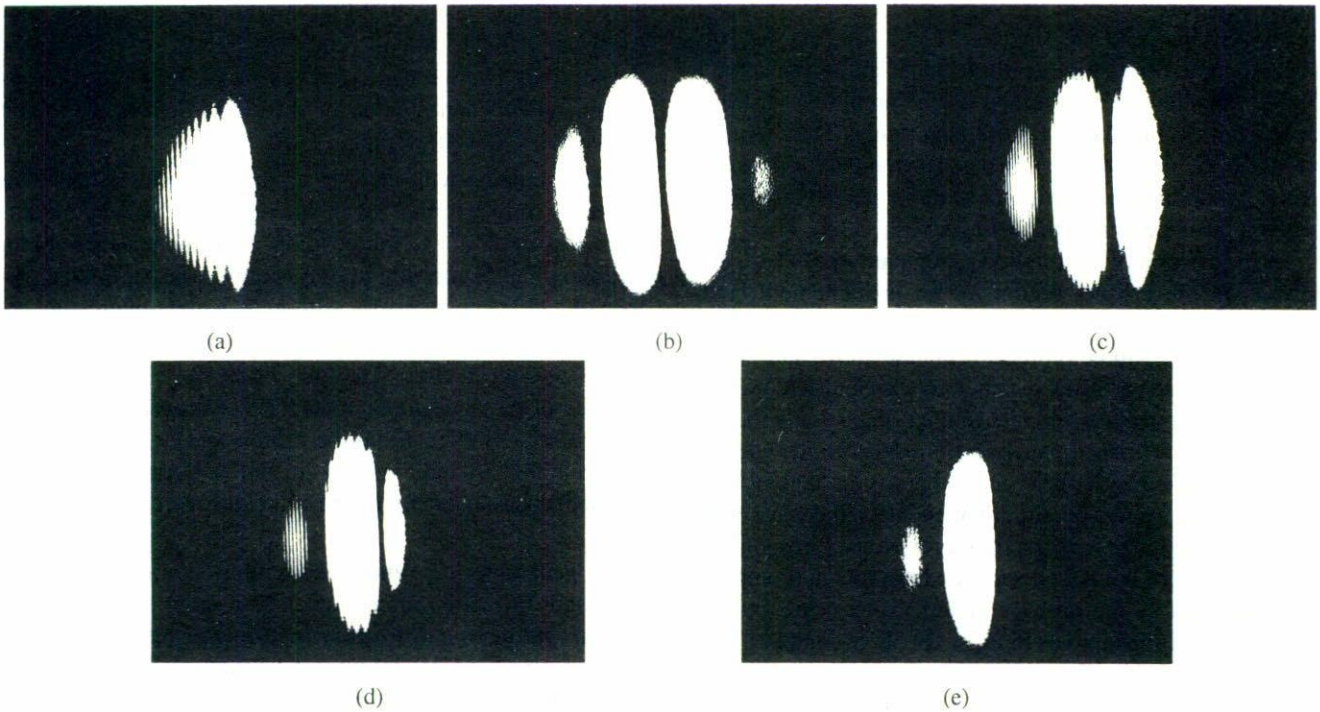

FIGURE 8. Experimentally obtained interference-diffraction patterns. (a) Fresnel diffraction of a single beam with Gaussian profile. In the set-up shown in Fig. 7, this is obtained with one mirror defeated. (b) Young fringes obtained with Gaussian profile beams propagating freely (no screen). The case corresponds to the thin trace shown in Figs. 5a-5d. (c) Edge at the maximum intensity. The case corresponds to Fig. 5b. (d) Edge at an intermediate value near one half-maximum. The case corresponds to Fig. 5c. (e) Edge at the minimum intensity. The case corresponds to Figs. 4b and 5d.

is illuminated by a spatially and temporally coherent source (at least to the degree obtainable with currently available gas lasers), non-localized fringes can be obtained which fill a certain volume of space. The interferometer was set up so as to have the contrast of the fringes approximately equal to one. Thus, the light intensity vanishes at the minima. An opaque straight edge diffracting screen is moved across the fringe pattern perpendicularly to the fringes and the field is observed at a point of coordinates (x_0, y_0, z). This produces the same effect as if the edge is maintained stationary and the initial phase α is varied from 0 to 2π.

In our experiment we collimated and expanded to 2 cm diameter the output beam of an unpolarized He-Ne laser operating at the fundamental Gaussian mode (TEM_{00}) and λ =594 nm. The interference angle is of the order of 2×10^{-4}rad. The observation plane was at a distance of 4 *meters* from the diffracting edge.

We should say a few words about the procedure for adjusting the elements. The experiment was performed on top of a holographic table providing vibration insulation to a certain degree. The optical equipment facilitated the needed positioning to micrometer accuracy in the linear dimensions. It also allowed us to fix the angular positions of the various elements employed in a reliable way to less than a degree accuracy. In determining the position for a minimum intensity we employed a computer aided CCD camera detection system which allowed us to monitor the diffraction patterns in real time. Nevertheless, for this presentation we employed photographic film to record the patterns because it offered graininess to a smaller extent. In practice the manual placement of the edge was performed while observing the diffracted light pattern. A symmetric pattern is associated with the edge being parallel to the fringes and vice-versa. Also the observation of the light scattered from the surface of the knife *near* the edge was used as an indicator of the proximity of the edge to the minimum intensity in the dark fringe.

Figure 8 shows the resulting intensity patterns for different positions of the edge. Figure 8a shows a normal Fresnel diffraction pattern of a normally incident Gaussian beam by a straight edge, for reference. Figure 8b corresponds to an undiffracted two beam interference pattern.

In Figs.8c–8e the pattern of Fig. 8b is diffracted by a straight edge whose position is varied according to:

Figure 8c edge at the peak of intensity (bright fringe). Figure 8d edge at an intermediate intensity near one half maximum. Figure 8e edge at nearly zero intensity (dark fringe)

Examination of Figs. 8c and 8d shows that a pattern is formed which contains interference and diffraction fringes. This is because both effects take place simultaneously.

In Fig. 8e the interference fringes remain and the diffraction fringes disappear. This pattern is equal to a truncated version of the undiffracted interference pattern shown in Fig. 8b. This is only for the case 8d and this conforms with theoretical results, see Fig. 5d.

4. Summary

In accordance with the Rayleigh-Sommerfeld formulation, a diffraction pattern is determined by the amplitude distribution of a field in the plane of diffracting screen. Thus, a rather different behavior of diffraction pattern is found for the cases when a maximum or a minimum of an interfered field is incident on the edge of the diffracting screen.

The diffraction by a straight edge opaque screen has been analyzed in the Fresnel region for an incident field composed by two coherent plane wavefronts for both constant and Gaussian amplitude profiles. From the above analysis, it is apparent that the diffraction pattern of two interfered waves is mainly determined by the interference angle θ and the position of the interference pattern with respect to the edge of the diffraction screen. Furthermore, there is an angle θ such that, in the case when a maximum of an interfered wave coincides with the edge of a diffraction screen, the corresponding diffraction pattern has a well separated prominent (comparable with that of an interference pattern) peak nearest to the shadow region (thick curves in Figs. 1b, 3b, 5c, and 8c).

The difference between diffraction patterns in the two cases, when a bright fringe ($\alpha = 0$) and a zero amplitude fringe ($\alpha = \pi$) of an interfered incident wave are located on the edge of the diffraction screen, has significantly appeared for small values of interference angle θ. In the case $\alpha = \pi$ and rather small $\theta \leq 2 \times 10^{-4}$ rad (see, for example, thick curves in Figs. 2a–2c, and Fig. 8d), a diffraction pattern is almost a replica of the corresponding interference pattern (thin curves in Figs. 2a–2c, and Fig. 8b), but the former has relatively small diffraction distortions. Increasing of θ decreases the separation between interference peaks, and in turn causes considerable penetration of the diffracted field in the region of geometrical shadow, plots 2b–2d.

The situation with the diffraction of interfered Gaussian beams is similar to that given above. The additional parameters, the width w and the position x_1 of the envelope of an interfered incident beam, mainly manifest through the envelope of a diffraction pattern. Although, a quite interesting redistribution of energy in the interference fringes caused by diffraction can be noticed in thick curve 5c.

One of the appealing situations is that posed by the fact that diffraction effects may be diminished or precluded, as shown in Fig. 8d and Figs. 2a–2c, and 4a–4c, under the condition that zero intensity fringe coincides with the diffracting edge.

In general terms, simultaneous consideration of interference and diffraction effects, even in a quite simple optical system, produces a *diffraction-interference* intensity pattern which features added degrees of freedom, among them the adjustable beam balance. The latter can be practically useful for purposes of controlling and correcting of diffraction effects in more complex situations than the one considered here (for example, by means of interference with some probe beams). Coupling of the two fundamental effects might find application in fringe enhancement or suppression - fringe manipulation, in general.

1. M. Born and E. Wolf, *Principles of Optics*, 5th edition (Pergamon Press, Oxford, 1975).
2. W.H. Steel, *Interferometry*, 2nd edition (Cambridge University Press, Cambridge, 1983).
3. J.W. Goodman, *Introduction to Fourier Optics*, (McGraw Hill, San Francisco, 1968).
4. R.S. Longhurst, *Geometrical and Physical Optics*, 3rd edition (Longman, London, 1973).
5. J.E. Pearson, T.C. McGill, S. Kurtin, and A. Yariv., *J. Opt. Soc. Am.* **59** (1969) 1440.
6. A.C. Livanos, and N. George, *Appl. Opt.* **14** (1975) 608.
7. T.D. Visser and S.H. Wiersma, *J. Opt. Soc. Am. A* **9** (1992) 2034.
8. G. Otis and J.W.Y. Lit, *Appl. Opt.* **14** (1975) 1156.
9. L.H. Tanner, *Appl. Opt.* **15** (1976) 857.
10. V.N. Mahajan, *J. Opt. Soc. Am. A* **3** (1986) 470.
11. I.S. Gradshteyn and I.M. Ryzhik, *Table of Integrals, Series, and Products*, 4th edition (Academic Press, London, 1980).
12. G.D. Boyd and J.P. Gordon, *Bell System Tech. J.* **40** (1961) 489.
13. H. Kogelnik, *Appl. Opt.* **4** (1965) 1562.
14. A. Yariv, *Quantum Electronics*, 3rd edition, Chap. 6 (John Wiley & Sons, Inc., N.Y., 1989).
15. G.D. Boyd and H. Kogelnik, *Bell System Tech. J.* **41** (1962) 1347.
16. A.G. Fox and T. Li, *Bell System Tech. J.* **40** (1961) 453.
17. P.K. Das, *Optical Signal Processing*, Chap. 2.8 (Springer-Verlag, Berlin, 1991)
18. D.B. Brayton, *Appl. Opt.* **13** (1974) 2346.